Petrological Evidence from Komatiites for an Early Earth Carbon and Water Cycle

Claude Herzberg*

Department of Earth and Planetary Sciences, Rutgers University, 610 Taylor Road, Piscataway, NJ 08854, USA

*E-mail: herzberg@rci.rutgers.edu

ABSTRACT

Komatiites from Alexo and Pyke Hill in the Archean Abitibi greenstone belt provide petrological evidence for an early Earth carbon and water cycle, ingassing in the cool Hadean and outgassing in the hot Archean. The komatiites have SiO_2 contents that are lower than those expected of advanced volatile-free melting of mantle peridotite. The SiO_2 misfit cannot be plausibly accounted for by variations in model Bulk-Earth peridotite composition, perovskite fractionation in a magma ocean, addition of chondrites, a source that had recycled crust added to it, or by chemical alteration during serpentinization. One possible resolution to the silica misfit problem is obtained if the komatiites from Alexo and Pyke Hill were partial melts of carbonated peridotite, a conclusion based on reasonable agreement between the major element compositions of komatiites (i.e. SiO_2, Al_2O_3, FeO, MgO, and CaO) and experimental melt compositions of carbonated peridotite. High-degree melts with olivine as the sole residual phase can have low SiO_2 contents owing to carbonate addition. Furthermore, a role for significant H_2O is indicated from recent olivine-hosted melt inclusion studies. More work is needed to constrain how much CO_2 and H_2O is required to resolve the SiO_2 misfit, and the *T–P* conditions of melting. Failure to do so imposes significant uncertainty in Archean mantle potential temperature and geodynamic interpretations. These uncertainties notwithstanding, the komatiites appear to be recording important degassing events in the Archean. Depending on the extent of volatile degassing, hydrous and CO_2-rich komatiites could have formed either in mantle plumes or in ambient mantle. Ingassing may have occurred in the Hadean when atmospheric CO_2 and H_2O were sequestered by reaction with impact ejecta, oceanic crust and mantle peridotite to produce carbonates and hydrous minerals. Parts of the Earth may have been sufficiently cool at some point in the Hadean to ingas the deep mantle, consistent with a variety of constraints from zircon and isotopic studies. Hydrous and CO_2-rich komatiites formed from 'carbonated wetspots' in mantle plumes or ambient mantle later in the Archean. The drop in komatiite production at the end of the Archean may be a record of significant purging of the mantle in volatiles, affecting biogenic methane production and the evolution of oxygen in the atmosphere.

Key words: peridotite; komatiite; carbon cycle; Archean; Hadean; Abitibi

INTRODUCTION

Komatiites of Archean age have a wide range of MgO contents that reflect the removal and accumulation of olivine during magmatic differentiation (Arndt, 1986; Arndt *et al.*, 2008). Various petrological methods exist to restore the parental magma composition from which olivine crystallized, and these typically yield MgO contents in the 26–30% range (Bickle, 1982; Nisbet *et al.*, 1993; Herzberg *et al.*, 2007; Arndt *et al.*, 2008; Puchtel *et al.*, 2009; Herzberg, 2011; Sobolev *et al.*, 2016); however, liquid MgO contents may have been as high as 34% in some cases (Arndt *et al.*, 2008; Robin-Popieul *et al.*, 2012).

It has long been known that the MgO content of a partial melt of volatile-free mantle peridotite is positively correlated with the temperature and pressure of partial melting (e.g. O'Hara, 1965; Nisbet *et al.*, 1993). If the primary magma erupts to the surface, then the

temperature at which olivine crystallizes (i.e. olivine liquidus temperature; $T^{Ol/L}$) will be related to its MgO content. There have been many parameterizations that permit the calculation of $T^{Ol/L}$ from magmatic MgO content (Bickle, 1982; Sugawara, 2000; Herzberg *et al.*, 2007; Herzberg & Asimow, 2015), and these typically yield 1550–1660 °C for Archean komatiites that erupted at the surface with 26–34% MgO. Assuming volatile-free conditions and comparison with mantle plume magmatism of Phanerozoic age (Herzberg *et al.*, 2007; Herzberg & Gazel, 2009), the Archean komatiites may have been the hottest magmas ever to have erupted on Earth. Based on the best currently available estimates for the temperature of ambient mantle, a hot mantle plume interpretation has been invoked to explain the high MgO contents of the komatiites (e.g. Jarvis & Campbell, 1983; Campbell *et al.*, 1989; Herzberg, 1992, 2004; Nisbet *et al.*, 1993; Arndt *et al.*, 2008; Puchtel *et al.*, 2009; Herzberg *et al.* 2010).

Experimental petrology has documented the effects of H_2O in suppressing solidus and liquidus temperatures, and a subduction alternative to mantle plumes has been proposed for Archean komatiites (Parman *et al.*, 1997; Grove & Parman, 2004). However, field, geochemical and petrological evidence for production of wet komatiites in Archean subduction zones is controversial and difficult to establish (Arndt, 2003; Arndt *et al.*, 2008; Robin-Popieul *et al.*, 2012; Puchtel *et al.*, 2013). Most recently, Sobolev *et al.* (2016) reported the presence of melt inclusions with high MgO contents and 0·6% H_2O.

Here, evidence is presented that shows that volatile-free melting of mantle peridotite is not consistent with the observed SiO_2 contents of aluminum-undepleted komatiites from the Pyke Hill and Alexo areas of the Abitibi greenstone belt. From a petrological point of view, these are amongst the simplest komatiites to understand. They contain primitive olivine compositions (i.e. Mg number = 94·5; Sobolev *et al.*, 2007, 2016), which indicate that olivine was the sole residuum phase in the mantle after extensive melting (Herzberg, 2004). They also have a whole-rock major element geochemistry that indicates that olivine was the dominant crystallizing phase near the surface (Arndt, 1986; Arndt *et al.*, 2008). Mass balance of primary komatiite and olivine compositions therefore constrains the SiO_2 content of the source. It is demonstrated that Pyke Hill and Alexo komatiites have SiO_2 contents that are lower than those expected of volatile-free melting of a peridotite source. I show that this SiO_2 misfit cannot be plausibly accounted for by variations in Bulk-Earth peridotite composition, a source that had experienced a prior stage of perovskite fractionation in a magma ocean, addition of chondrites, or by chemical alteration during serpentinization. A role for magmatic volatiles is implicated by experimental data for carbonated peridotite (Dasgupta *et al.*, 2007, 2013) and elevated H_2O contents in olivine-hosted melt inclusions (Sobolev *et al.*, 2016). Results suggest that the mantle plume interpretation for the Archean komatiites from Pyke Hill and Alexo is not unique, and implications for an early Earth carbon and water cycle are discussed.
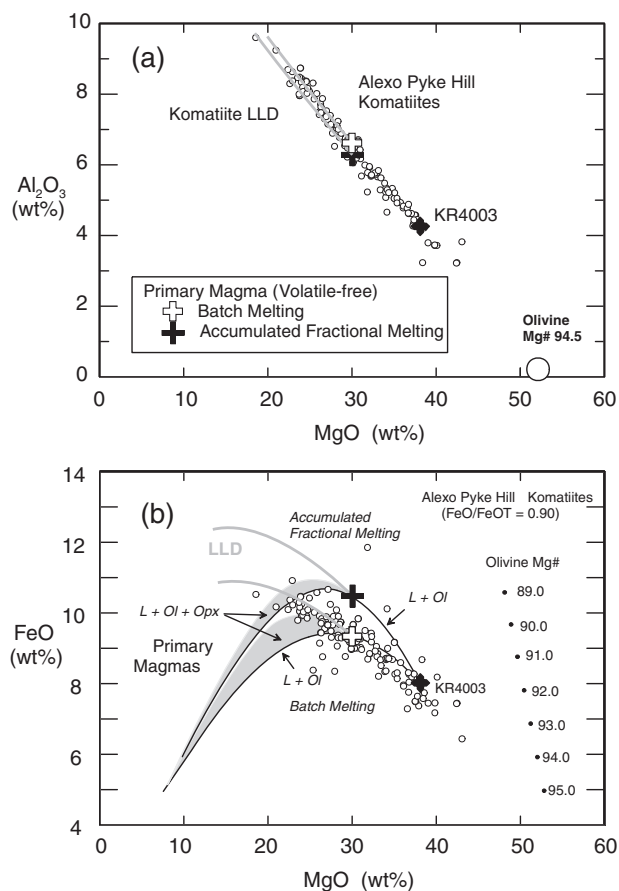
ARCHEAN KOMATIITES FROM ALEXO AND PYKE HILL AND THEIR PERIDOTITE SOURCE

Major element geochemistry
Peridotite KR4003 is used to model the compositions and formation of Archean komatiites from Alexo and Pyke Hill because there is a comprehensive set of melting experiments (Walter, 1998) and their parameterizations (Herzberg & O'Hara, 2002; Herzberg, 2004; Herzberg & Asimow, 2015). The parameterizations are mass-balance solutions to the compositions of primary magmas solved for equations appropriate for both accumulated fractional melting and batch melting. Model primary magma compositions for KR4003 were provided in appendices by Herzberg & O'Hara (2002) and Herzberg (2004), and they will be used again in the discussion that follows. Walter (1998) reported a whole-rock composition for KR4003 with 37·3% MgO, but the total is low (i.e. 99·18%) and the Mg-number for this composition is 89·2, in contrast to 89·5 for olivine in subsolidus experiment 60.02. An MgO content of 38·12% for KR4003 is more likely (Herzberg & O'Hara, 2002), because it brings the total to 100%, raises its Mg-number to 89·4, and predicts 89·4–89·5 for solidus olivine Mg-number, in better agreement with experiments. Peridotite KR4003 is only moderately depleted in Al_2O_3 and CaO with respect to the McDonough & Sun (1995) pyrolitic mantle; this is consistent with a residue that remained after only about 2% basalt extraction, and it is consistent with light rare earth element depletions and εNd values of + 2·9 by the time of komatiite emplacement at 2·7 Ga (Puchtel *et al.*, 2009).

The 2·7 Ga komatiites from the Alexo locality in the Abitibi greenstone belt are located close to those from Pyke Hill; they are aluminum-undepleted type komatiites in that they have Gd/Yb and Al_2O_3/TiO_2 indicative of derivation from high-degree melts of a primitive mantle source (e.g. Arndt *et al.*, 2008; Puchtel *et al.*, 2009). A database has been compiled (Arndt, 1986; Lahaye & Arndt, 1996; Shore, 1996; Fan & Kerrich, 1997; Sproule *et al.*, 2002; Puchtel *et al.*, 2004), and Fig. 1a shows that it defines a tight igneous trend in MgO–Al_2O_3 projection space, which terminates at olivine having the maximum Mg number of 94·5 as measured by high-precision electron microprobe analysis (Fig. 1a; Sobolev *et al.*, 2007, 2016). This trend is coincident with computed liquid lines of descent from model primary komatiites with 30% MgO (Herzberg *et al.*, 2007; Sobolev *et al.*, 2016), derived by either batch or accumulated fractional melting of peridotite KR-4003 as discussed more fully below.

Komatiites also display a trend towards olivine with an Mg number of 94·5 in MgO–FeO projection space (Fig. 1b). The best fit to the komatiites is obtained

Fig. 1. (a, b) MgO, FeO, and Al₂O₃ contents of komatiites from Alexo and Pyke Hill compared with their model volatile-free primary magma compositions and liquid lines of descent. The primary magmas, indicated by the white and black filled crosses, contain 30% MgO (Herzberg *et al.*, 2007; Herzberg, 2011; Sobolev *et al.*, 2016), and the Al₂O₃ and FeO contents are solutions to the primary magma problem using the equations for batch and accumulated fractional melting for peridotite KR4003 (Herzberg & O'Hara, 2002). All MgO–FeO primary magma solutions for dunite (L + Ol) and harzburgite (L + Ol + Opx) residua are from Herzberg & O'Hara (2002). The calculated liquid lines of descent are appropriate for fractional crystallization of olivine at the surface using FeO–MgO partitioning between olivine and liquid from Toplis (2005). Small open circles, whole-rock data for Alexo and Pyke Hill komatiites referenced in the text.

with a primary magma produced by batch melting, not accumulated fractional melting. The FeO contents of primary magmas produced by accumulated fractional melting are always higher that those produced by batch melting as long as the melts are not constrained by the solidus (Langmuir *et al.*, 1992; Herzberg & O'Hara, 2002). However, the inference of batch melting for the komatiites is based on the assumption that FeO/FeOT = 0·90 as measured by Berry *et al.* (2008) on komatiite olivine-hosted melt inclusions from the Belingwe greenstone belt in Zimbabwe. If the primary melts of the Alexo and Pyke Hill komatiites formed by accumulated fractional melting of peridotite KR4003, then all iron would have to be completely reduced (i.e. FeO/FeOT =

1·0) to obtain a good match. However, this is not compatible with more oxidized conditions inferred for komatiites (Canil, 1997; Berry *et al.*, 2008; Sobolev *et al.*, 2016). Alternatively, accumulated fractional melting might be compatible with a peridotite source that was intrinsically low in FeO compared with most peridotite compositions, which typically contain 8% FeO (Jagoutz *et al.*, 1979; Herzberg, 1993; McDonough & Sun, 1995; Palme & O'Neill, 2003; Workman & Hart, 2005; Jackson & Jellinek, 2013). Petrological models of primary magma generation at the present day recognize the importance of fractional melting (e.g. Langmuir *et al.*, 1992; Herzberg & Asimow, 2015). However, the physics of Archean komatiite melt generation might have been biased towards batch melting if pressures were high and the densities of primary melt and olivine became similar (Ohtani, 1985; Agee, 1998; Herzberg, 2004; Robin-Popieul *et al.*, 2012). Uncertainties about the melting mechanism notwithstanding, these models support the interpretation that the MgO, FeO and Al₂O₃ contents of the komatiites were established by igneous processes, and that they remained immobile during a subsequent period of greenschist-facies metamorphism (Arndt *et al.*, 2008).

Evidence for volatile-free melting

As examined more fully below, olivine phenocrysts with Mg numbers as high as 94·5 (Sobolev *et al.*, 2007) most probably crystallized from primary magmas that were formed by extensive melting of mantle peridotite, leaving behind only olivine as a residual phase (Herzberg, 2004). Mass balance with respect to KR4003 indicates that the primary magma had about 30% MgO and formed from 63% volatile-free melting of peridotite KR4003. A model volatile-free batch primary magma with 30% MgO also has 9·3% FeO, and 6·6% Al₂O₃ (Herzberg & O'Hara, 2002; Herzberg, 2004; Sobolev *et al.*, 2016), and is similar to many komatiites from Alexo and Pyke Hill (Figs. 1a and b); it also agrees with many other suggested primary komatiite magma compositions (Nisbet *et al.*, 1993; Arndt *et al.*, 2008; Puchtel *et al.*, 2009; Sobolev *et al.*, 2016). Using Fe–Mg exchange between olivine and melt (i.e. K_D from Toplis (2005) predicts that the primary magma would crystallize olivine at the surface with an Mg-number of 95·1, slightly higher than the 94·5 reported by Sobolev *et al.* (2007). This difference in olivine Mg number arises from the effect of elevated temperature and pressure on increasing K_D (Toplis, 2005). The calculated olivine liquid line of descent reproduces very well those komatiites with MgO contents lower than 30%; komatiites with MgO contents higher than 30% experienced olivine accumulation. In summary, the evidence from MgO, FeO, and Al₂O₃ is that the Alexo and Pyke Hill komatiites are consistent with extensive volatile-free melting of a peridotite similar in composition to KR4003.

Evidence against volatile-free melting

Figure 2a shows that the model primary magma for Alexo and Pyke Hill komatiites has a slightly lower CaO content than observed. The komatiite trend does not extend to olivine with an Mg-number of 94·5, nor does it coincide with the calculated liquid line of descent. This is a demonstration of Ca mobility during greenschist-facies metamorphism, a problem that has been previously recognized (Herzberg, 1992; Lahaye *et al.*, 1995; Lahaye & Arndt, 1996; Arndt *et al.*, 2008; Puchtel *et al.*, 2009). It is possible that Ca lost from MgO-rich cumulates may have been gained by the MgO-poor derivative rocks.

As shown in Fig. 2b, the Alexo and Pyke Hill komatiites have lower SiO_2 contents than the model primary magma computed for volatile-free melting of peridotite KR4003. This misfit is shown again in Fig. 3, where the MgO and SiO_2 contents of the komatiites are compared with those that have been calculated for volatile-free primary melts of KR4003 produced by both batch and accumulated fractional melting; the misfit is greater for batch melting compared with accumulated fractional melting, but the FeO contents of the komatiites are more consistent with batch melting (Fig. 1b). Figure 3a is a parameterization (Herzberg, 2004) of the experimental data of Walter (1998) and it can be seen that the agreement is excellent. Figure 3 also includes the compositions of the olivines that are expected to crystallize from the primary magmas at the surface, calculated using the Toplis (2005) model for K_D; the primary magma composition shown by the white cross in Fig. 2b is shown again in Fig. 3a. Compared with the komatiites, the range of possible volatile-free primary magma compositions that would crystallize olivine with Mg-numbers of 94·5 (Sobolev *et al.*, 2007, 2016) is higher in SiO_2, and most consistent with olivine as the sole residuum phase. In contrast, the primary magma composition of Sobolev *et al.* (2016) with 30% MgO is located in MgO–SiO_2 projection space defined by the melting of garnet peridotite, not harzburgite or dunite; residual garnet peridotite is not consistent with the geochemistry of the Alexo and Pyke Hill komatiites (e.g. Arth *et al.*, 1977; Herzberg, 1992; Walter, 1998; Arndt *et al.*, 2008; Puchtel *et al.*, 2009). A komatiite primary magma with 30% MgO is too low in SiO_2 by 1–2% compared with volatile-free batch or accumulated primary melts of mantle peridotite. Possible solutions to the SiO_2 misfit are now examined and discounted, as follows.

(1) The komatiites formed from a peridotite composition that had a lower SiO_2 content than KR4003. Shown in Fig. 4 are different silicate Earth models and moderately depleted peridotite compositions compared with KR4003 (Jagoutz *et al.*, 1979; Ringwood, 1979; Wänke *et al.*, 1984; Hart & Zindler, 1986; McDonough & Sun, 1995; Allègre *et al.*, 1995; Palme & O'Neill, 2003; Workman & Hart, 2005; Lyubetskaya & Korenaga, 2007; Davis *et al.*, 2009; Jackson & Jellinek, 2013). None of
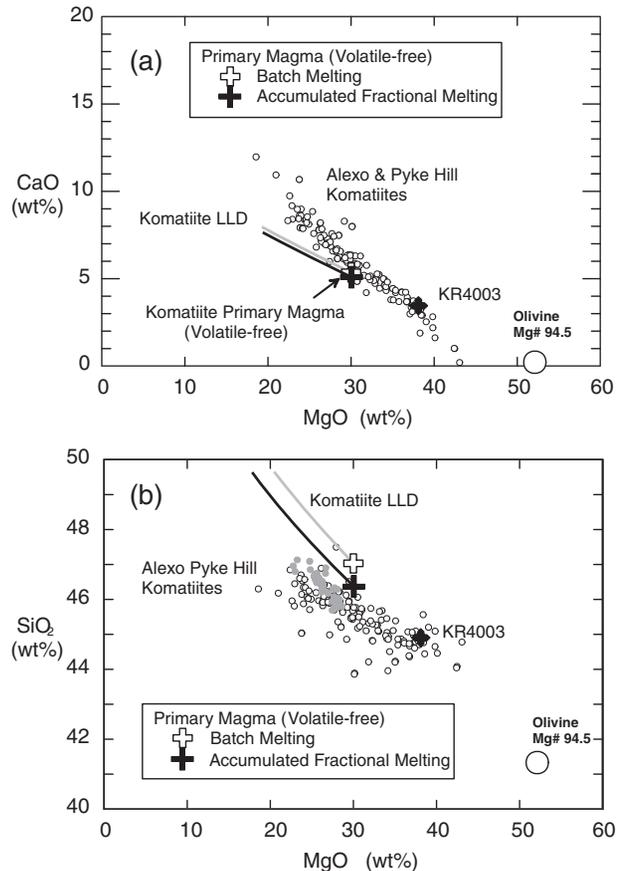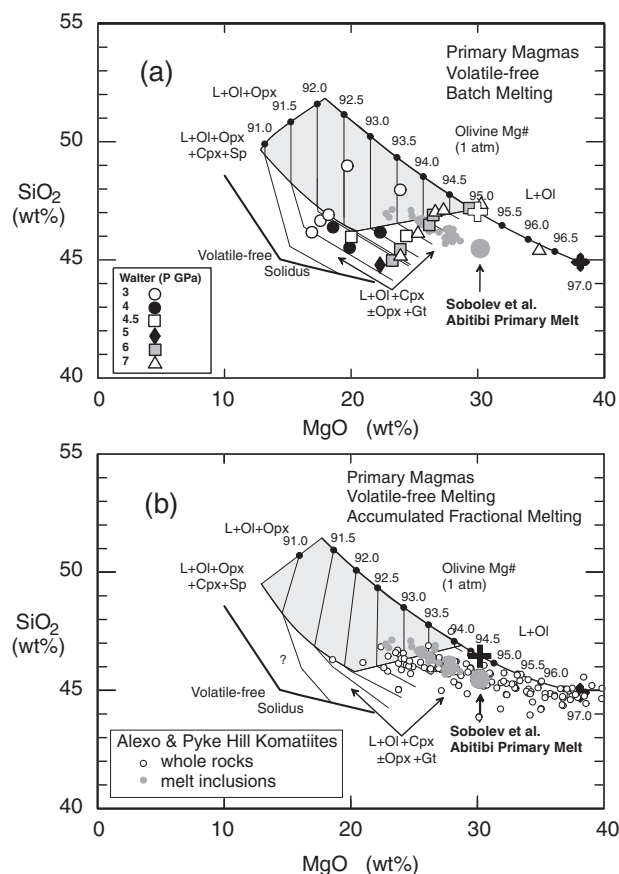

Fig. 2. (a, b) MgO, CaO, and SiO_2 contents of komatiites from Alexo and Pyke Hill compared with their model volatile-free primary magma composition and its liquid line of descent. The primary magmas, indicated by the white and black filled crosses, contain 30% MgO (Herzberg *et al.*, 2007; Herzberg, 2011; Sobolev *et al.*, 2016), and the CaO and SiO_2 contents are solutions to the primary magma problem using the equations for batch and accumulated fractional melting for peridotite KR4003 (Herzberg & O'Hara, 2002). The model volatile-free primary magma compositions and their liquid lines of descent are nearly linearly connected with peridotite KR4003 and olivine with an Mg number of 94·5, the maximum for olivines from Alexo komatiites (Sobolev *et al.*, 2007). Alexo and Pyke Hill komatiites are too low in SiO_2 to have crystallized from the model primary magma; the trend towards KR4003 is an artefact of SiO_2 addition during metamorphic alteration, and has no igneous significance. Small open circles, whole-rock data for Alexo and Pyke Hill komatiites referenced in the text; small grey filled circles, melt inclusions (Sobolev *et al.*, 2016).

these alternative models have sufficiently low SiO_2 compositions to solve the SiO_2 misfit problem, and most of them are too high in SiO_2.
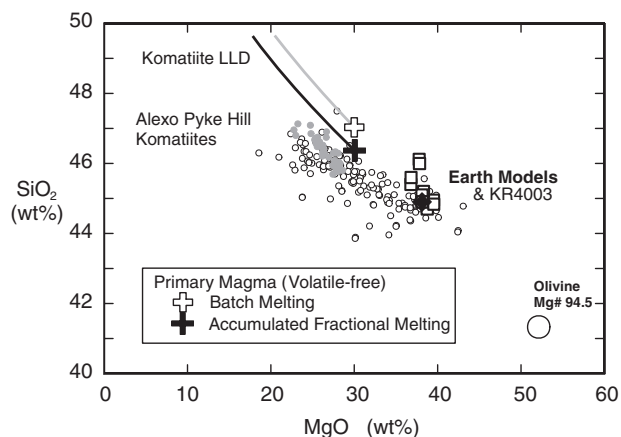
(2) The komatiite source differed from most model Earth compositions owing to addition of chondrites. This idea is not consistent with the elevated SiO_2 contents of chondrites (e.g. Jagoutz *et al.*, 1979).

(3) The komatiites did not melt from peridotite, but from a source that contained a substantial amount of recycled crust. This is not consistent with the olivine phenocryst compositions of Alexo komatiites (Sobolev *et al.*, 2007), which have Ni, Ca, and Mn contents that record a peridotite source lithology (Herzberg, 2011).

Fig. 4. MgO and SiO$_2$ contents of komatiites from Alexo and Pyke Hill compared with model volatile-free primary melts of peridotite KR4003, shown by the black filled cross. Other possible source peridotite compositions are shown as the open squares, but they do not provide a better solution to the problem of understanding the SiO$_2$ contents of komatiites from Alexo and Pyke Hill. Other symbols as in Fig. 3

Fig. 3. MgO and SiO$_2$ contents of komatiites from Alexo and Pyke Hill compared with model volatile-free primary magmas of peridotite KR4003 produced by batch melting (a) and accumulated fractional melting (b), and the Mg-numbers of olivine that would crystallize at 1 atm. The model batch primary magma with 30% MgO and in equilibrium with olivine only (L + Ol), shown as the white filled cross, is from Fig. 2b. Small open circles, whole-rock data sources as in the text; small grey filled circles, melt inclusions (Sobolev *et al.*, 2016); large grey circle, average primary magma composition of Sobolev *et al.* (2016). (a) Experimental results of Walter (2008) and their parameterization for primary magmas formed by volatile-free batch melting (Herzberg & O'Hara, 2002; Herzberg, 2004). (b) Model primary magma compositions formed by volatile-free accumulated fractional melting (Herzberg, 2004) compared with whole-rock and melt inclusions from Alexo and Pyke Hill komatiites. The model accumulated primary magma with 30% MgO and in equilibrium with olivine only (L + Ol) shown as the black filled cross is from Fig. 2b.

(4) The komatiites melted from a peridotite composition that had a lower SiO$_2$ content than KR4003 because of fractionation of a SiO$_2$-rich phase such as magnesium perovskite in a magma ocean (Herzberg & O'Hara, 1985; Ohtani, 1985). Using magnesium perovskite compositions reported by Trønnes & Frost (2002), synthesized at 24.5 GPa, it can be shown that 10% Mg-perovskite fractionation may indeed yield a peridotite composition with sufficiently low SiO$_2$; however, this process drives up FeO to high levels, and would predict FeO contents of komatiites that are higher than observed. Also, Mg- and Ca-perovskite fractionation has been predicted to result in the decoupling of the

Nd–Hf systematics in the Abitibi komatiite source, which is not observed (Blichert-Toft & Puchtel, 2010).

(5) The komatiites formed by volatile-free melting, and SiO$_2$ is low owing to a subsequent stage of metamorphic alteration. Recent work on the serpentinization of abyssal peridotite indicates that this explanation is not likely. Low-temperature metamorphism should yield serpentine [Mg$_3$Si$_2$O$_5$(OH)$_4$] and brucite [Mg(OH)$_2$], in addition to magnetite. However, brucite is rarely observed in serpentinized abyssal peridotite (Malvoisin, 2015). Serpentinization is not an isochemical process, and Malvoisin (2015) proposed that brucite is lost by reaction with aqueous Si-rich fluids to make more serpentine. That is, the effect of serpentinization is to increase SiO$_2$ content rather than lower it. If the open-system serpentinization model of Malvoisin (2015) is generally applicable to magnesium-rich rocks, then it would have resulted in SiO$_2$ gain in komatiites, not SiO$_2$ loss, and this has probably affected those Abitibi komatiite compositions with MgO contents near 40% (Fig. 2b; see also Lahaye & Arndt, 1996). Importantly, recent work by Sobolev *et al.* (2016) shows that the SiO$_2$ contents of olivine-hosted melt inclusions are about 46% at 28% MgO, very similar to those of the whole-rocks. For parental magmas with 30% MgO, the SiO$_2$ content is 45.5%, again similar to the whole-rock compositions (Fig. 3b).

There is a persistent misfit between predicted SiO$_2$ expected for volatile-free melting and observed SiO$_2$ contents. Evidence is now presented that it may be resolved by volatile-melting of peridotite.

Evidence for carbonated peridotite melting

Two melt compositions are shown in Fig. 5, A496 and M354, synthesized from experiments on a carbonated peridotite composition PERC (Dasgupta *et al.*, 2007,
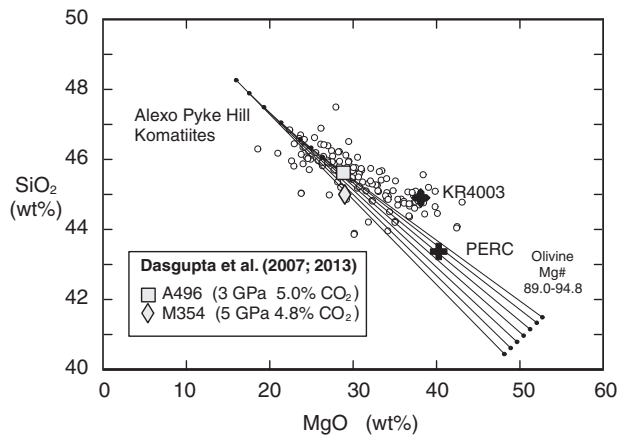
Fig. 5. MgO and SiO_2 contents of komatiites from Alexo and Pyke Hill compared with CO_2-free normalized experimental melt compositions A496 and M354 of Dasgupta *et al.* (2007, 2013) for carbonated peridotite PERC. The composition indicated by the square is melt composition A496, assumed to be a primary magma composition for the komatiites. Addition and subtraction of olivine at the surface from experimental melt A496 yields a liquid line of descent and olivines in equilibrium with the liquid line of descent; there is generally good agreement with the komatiites, but the higher SiO_2 contents of komatiites can be interpreted as silica gain during metamorphic alteration (Malvoisin, 2015).

2013). They are the highest-temperature and highest-degree melts in these studies, olivine is the sole residual phase, and they contain about 5 wt % dissolved CO_2. However, the melt compositions reported and shown were normalized to a carbon-free basis; in this sense, they may represent degassed and decarbonated melt compositions. PERC has 2·5 wt % CO_2 and was synthesized by adding carbonates to a peridotite composition; its SiO_2 content is lower than that of KR4003 by 1·5 wt % (Fig. 5). The melt compositions A496 and M354 have low SiO_2 contents that reflect carbonate addition, they have 29% MgO normalized CO_2-free, and they coexist with olivine with an Mg-number of 93·4, similar to some olivines in Alexo and Pyke Hill komatiites (Sobolev *et al.*, 2007, 2016). If these melt compositions were to erupt to the surface and degass all their CO_2, they would crystallize olivine with an Mg-number of 94·8, based on the effect of pressure on the Fe–Mg olivine–liquid exchange model of Toplis (2005); such high Mg-numbers are similar to the maxima that have been measured in olivines from Alexo (Sobolev *et al.*, 2007, 2016). Fractional crystallization of olivine from the experimental melt composition A496 would yield an array of rock compositions defined by the liquid line of descent, olivine compositions, and olivine cumulate mixtures; this array is similar in composition to many Alexo and Pyke Hill komatiites with MgO contents <30% MgO (Fig. 5). Calculated SiO_2 contents are somewhat lower than observed komatiite compositions at 30–40% MgO, a misfit that is reasonably accounted for by serpentinization (Malvoisin, 2015). The CO_2-free

normalized experimental melts compositions A496 and M354 of Dasgupta *et al.* (2007, 2013) are therefore possible primary magma compositions for Alexo and Pyke Hill komatiites. These experimental melt compositions, their calculated liquid lines of descent and olivine compositions yield arrays with CaO, Al_2O_3 and FeO contents that are also similar to those of the Alexo and Pyke Hill komatiites (Fig. 6). This is evidence for the potential importance of carbonated peridotite melting in the formation of these komatiites.

Evidence for hydrous peridotite melting

If komatiites contained CO_2 then we may reasonably guess that they also contained H_2O. The hydrous experiments of Parman *et al.* (1997) and Parman & Grove (2004) were conducted on picrite and komatiite compositions, not peridotite, and therefore do not help to constrain the SiO_2 content of the peridotite source. Data are available on the melting of hydrous peridotite KLB-1 at 3·5, 12, and 13 GPa (Tenner *et al.*, 2012*a*, 2012*b*), and synthesized melt compositions are in equilibrium with Ol + Opx ± Cpx ± Gt. No H_2O-bearing experiments have been reported having olivine as the sole residual phase appropriate to the Alexo and Pyke Hill komatiites. Like CO_2 (Dasgupta *et al.*, 2007, 2013), experiments on hydrous peridotite (Tenner *et al.*, 2012*a*) at high pressures show that the effect of H_2O is to expand the stability field of L + Ol + Opx with respect to L + Ol + Opx + Gt, and this will drive SiO_2 content down. In the extreme, large amounts of water can yield low-SiO_2 kimberlite-like partial melts (Kawamoto & Holloway, 1997). In general, melting with CO_2 and H_2O at high pressure will lower the SiO_2 content of partial melts relative to volatile-free peridotite melting; future experiments on mixed CO_2–H_2O volatiles may provide better constraints on the komatiite problem. The interpretation that experiments A496 and M354 are reasonable primary komatiite compositions is therefore unlikely. There may be a broad range of CO_2–H_2O contents, and the temperature and pressure conditions of melting for komatiite production in nature may have been very different from experiments A496 and M354.

Analysis of olivine-hosted melt inclusions from Alexo and Pyke Hill komatiites shows that CO_2 contents vary from 100 to 400 ppm, and H_2O contents vary from 0·1 to 0·8 wt % when corrections have been made for olivine and spinel crystallization, Fe–Mg exchange between melt inclusion and host olivine, and CO_2 in shrinkage bubbles (Sobolev *et al.*, 2016). Sobolev *et al.* inferred minor degassing because of agreement in H_2O-corrected olivine liquidus temperatures determined by Fe–Mg and Sc/Y partitioning between olivine and melt. However, this agreement simply means that the CO_2 and H_2O contents are those appropriate for the trapped parental magma at the time of olivine crystallization. If the volatile contents of the primary magmas from the mantle were higher, then degassing may have been
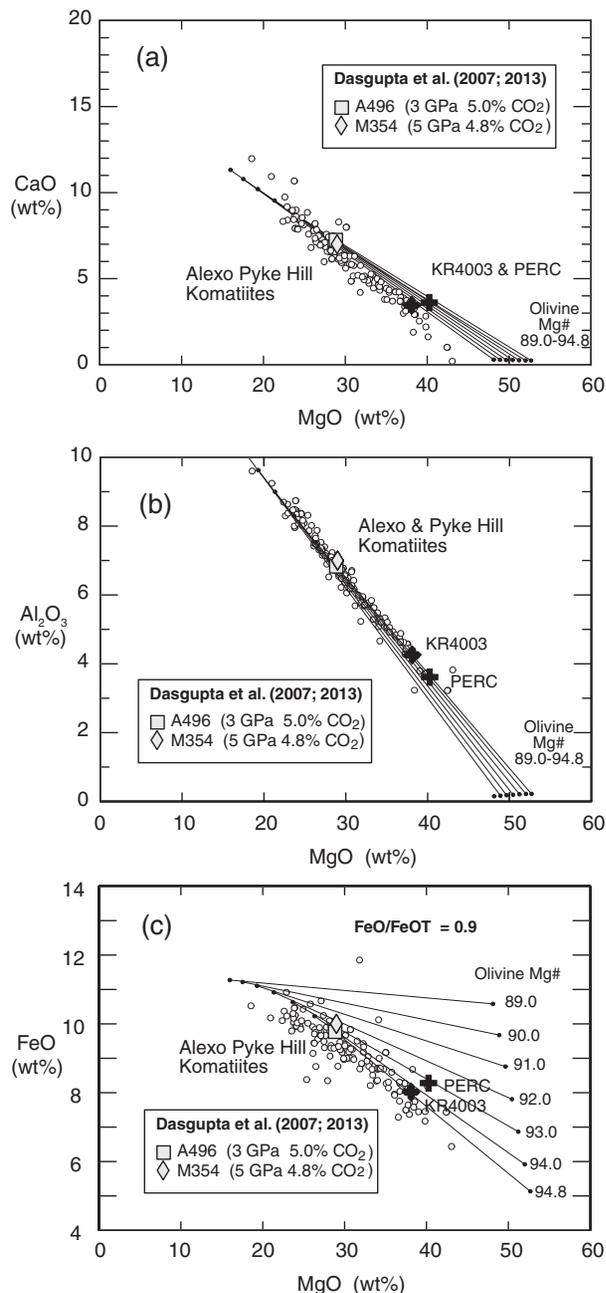
Fig. 6. MgO, CaO, Al$_2$O$_3$ and FeO contents of komatiites from Alexo and Pyke Hill compared with CO$_2$-free normalized experimental melt compositions A496 and M354 of Dasgupta *et al.* (2007, 2013) for carbonated peridotite PERC. As in Fig. 5, the composition indicated by the square is experimental melt composition A496, assumed to be a primary magma composition for the komatiites. There is generally good agreement between komatiite compositions and model compositions produced by addition and subtraction of olivine from A496. Equilibrium olivine compositions are tied to liquids along the liquid line of descent, and crystallize at 1 atm.

extensive prior to olivine crystallization, and the volatile contents reported by Sobolev *et al.* (2016) represent minimum bounds on the CO$_2$ and H$_2$O contents of primary magmas from the mantle source.

Volatile contents of parental and primary komatiite magmas

Melt inclusion and experimental studies will provide contrasting information about source volatile contents owing to variable degassing. As an example, if the experimental melt composition A496 of Dasgupta *et al.* (2007) is a reasonable model primary komatiite magma and it were to erupt somehow without degassing, then it would have had ~5·0 wt % CO$_2$ and 43·4 wt % SiO$_2$; however, CO$_2$ solubility in magmas is low at low pressures, and if CO$_2$ was totally degassed then the primary magma would have 45·6% SiO$_2$. In either case, the SiO$_2$ content is lower than that expected of volatile-free melting (Figs 2 and 3). Consequently, partial degassing of CO$_2$, and by analogy H$_2$O, will yield parental melt inclusion volatile contents that can be much lower than those inferred from the SiO$_2$ contents of the primary magmas in the mantle. In this sense, it is important to distinguish parental from primary magmas, and they do not always have identical compositions (Herzberg *et al.*, 2007). In theory, the SiO$_2$ contents and perhaps other major elements of komatiites can preserve the memory of primary magma volatile content that is otherwise lost to degassing. However, in practice, the experimental melt compositions A496 and M354 of Dasgupta *et al.* (2007, 2013) are only suggestive of a wide range of CO$_2$–H$_2$O and *T–P* possibilities that have yet to be explored experimentally. There is at present great uncertainty about the volatile content of the primary komatiite magma and its peridotite source, and this has profound geodynamic implications, which are discussed next.

Effects of volatiles on olivine liquidus temperature and mantle potential temperature

Although primary magma volatile contents are uncertain, it is instructive to consider how the range of possibilities will affect inferences concerning olivine liquidus temperature and mantle potential temperature. A parameterization of volatile-free (vf) nominally anhydrous and decarbonated experimental olivine liquidus temperatures yields

$$T_{vf,1}^{Ol/L} = 1020 + 24·4MgO - 0·161MgO^2 \qquad (1)$$

(Herzberg & Asimow, 2015) where $T_{vf,1}^{Ol/L}$ is the volatile-free olivine liquidus temperature at 1 atm (in °C), and MgO is the MgO content (in wt %) of the magma; this can be extended to higher pressures using the equation

$$T_{vf,P}^{Ol/L} = T_{vf,1}^{Ol/L} + 54P - 2P^2 \qquad (2)$$

where $T_{vf,P}^{Ol/L}$ is the olivine liquidus temperature at *T* and pressure *P* (in GPa), and $T_{vf,1}^{Ol/L}$ is defined in equation (1) (Herzberg & O'Hara, 2002; Putirka *et al.*, 2007; Herzberg & Asimow, 2015).

There are many parameterizations that have calibrated the effect of H$_2$O on olivine liquidus temperature depression for basaltic compositions (Falloon & Danyushevsky,

2000; Putirka, 2008). Here the effect of H_2O and CO_2 addition on lowering the olivine liquidus temperature has been examined using a self-consistent set of hydrous and carbonated experiments on peridotite KLB-1 at a wide range of T–P conditions in the mantle (Dasgupta *et al.*, 2007, 2013; Tenner *et al.*, 2012*a*, 2012*b*). It is useful to compare these experimental conditions with the 1 atm nominally volatile-free reference frame described by equation (1). For each volatile experiment a calculation is made of the 1 atm metastable zero degassing condition using the olivine liquidus pressure terms:

$$T_{H2O,CO2,1}^{Ol/L} = T_{H2O,CO2,P}^{Ol/L} - (54P - 2P^2) \qquad (3)$$

where $T_{H2O,CO2,P}^{Ol/L}$ is the olivine liquidus temperature measured in the experiments at pressure P (in GPa). The term $T_{H2O,CO2,1}^{Ol/L}$ is simply a way to calculate the experimental olivine liquidus temperature at 1 atm, and to compare it with the volatile-free condition at 1 atm:

$$\Delta T^{Ol}_1 = T_{vf,1}^{Ol/L} - T_{H2O,CO2,1}^{Ol/L}. \qquad (4)$$

As shown in Fig. 7a, increased H_2O and CO_2 dissolved in the experimental melts suppress the olivine liquidus temperature as described by larger values of ΔT^{Ol}_1. The effect of H_2O on lowering olivine liquidus temperature is much greater than that of CO_2, and there are significant pressure effects.

Primary magmas formed in a hot mantle with elevated mantle potential temperature TP must also crystallize olivine at high liquidus temperatures should they erupt at the surface. The relationship between volatile-free mantle potential temperature TP_{vf} and olivine liquidus temperature at 1 atm $T_{dry,1}^{Ol/L}$ can be represented by the equation

$$TP_{vf} = 1 \cdot 049 T_{vf,1}^{Ol/L} - 0 \cdot 00019 (T_{vf,1}^{Ol/L})^2 + 1 \cdot 487 \times 10^{-7} (T_{vf,1}^{Ol/L})^3 \qquad (5)$$

(Herzberg & Asimow, 2015). And for volatile-free (vf) nominally anhydrous and decarbonated peridotite

$$TP_{vf} = 1025 + 28 \cdot 6MgO - 0 \cdot 084MgO^2 \qquad (6)$$

(Herzberg & Asimow, 2015). We can now explore the effects of H_2O and CO_2 addition on mantle potential temperature. For each volatile experiment we calculate the mantle potential temperature using equation (5) and rewriting it as

$$TP_{H2O,CO2} = 1 \cdot 049 T_{H2O,CO2,1}^{Ol/L} - 0 \cdot 00019 (T_{H2O,CO2,1}^{Ol/L})^2 + 1 \cdot 487 \times 10^{-7} (T_{H2O,CO2,1}^{Ol/L})^3. \qquad (7)$$

Increased H_2O and CO_2 dissolved in the experimental melts suppress mantle potential temperature relative to the volatile-free condition by

$$\Delta TP = TP_{vf} - TP_{H2O,CO2} \qquad (8)$$
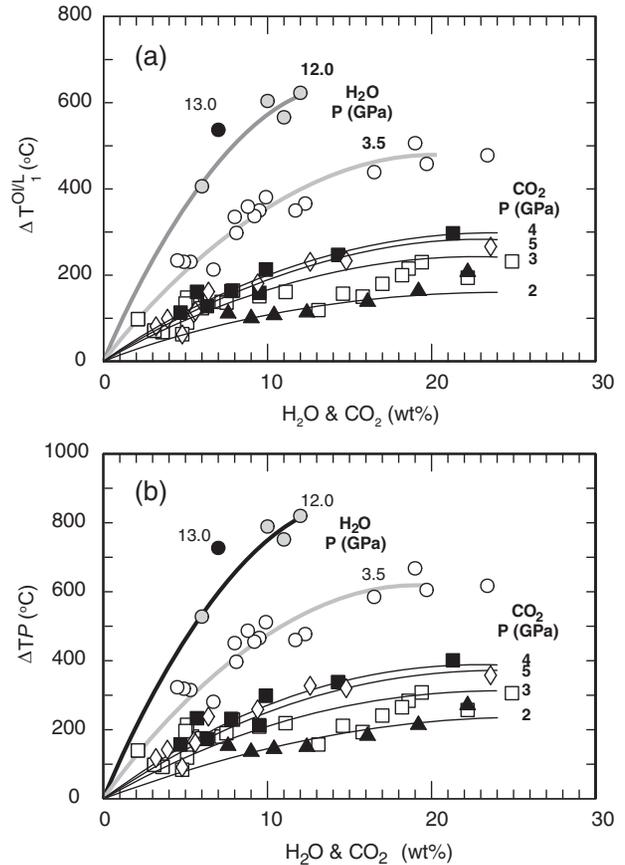
Fig. 7. Depressions in olivine liquidus temperature at 1 atm (ΔT^{Ol}_1) and mantle potential temperature (ΔTP) arising from addition of H_2O and CO_2 to mantle peridotite. Circles indicate H_2O-bearing experiments of Tenner *et al.* (2012*a*, 2012*b*): white, 3·5 GPa; grey, 12·0 GPa; black, 13·0 GPa. Other symbols indicate CO_2-bearing experiments of Dasgupta *et al.* (2007, 2013): black triangles, 2 GPa; white squares, 3 GPa; black squares, 4 GPa; white diamonds, 5 GPa. Curves are parameterizations of these data using equations (9) and (10) and constants given in Table 1.

where TP_{vf} and $TP_{H2O,CO2}$ are given in equations (6) and (7). Results of ΔTP calculated from experiments on peridotite KLB-1 (Dasgupta *et al.*, 2007, 2013; Tenner *et al.*, 2012*a*, 2012*b*) are shown in Fig. 7b.

The effects of H_2O and CO_2 on the ΔT terms have been parameterized using the equations

$$\Delta T^{Ol}_1 = a(H_2O, \ CO_2) + b(H_2O, \ CO_2)^2 \qquad (9)$$
$$\Delta T^{Ol}_1 = c(H_2O, \ CO_2) + d(H_2O, \ CO_2)^2 \qquad (10)$$

and the constants a, b, c, and d are listed in Table 1. These parameterizations are generally successful in describing the experimental data to within $\pm <100\,°C$; for the CO_2-rich komatiitic compositions of Dasgupta *et al.* (2007, 2013), the maximum difference between calculated and measured CO_2 yields $T < 80\,°C$. An evaluation is now made concerning how much magmatic H_2O and CO_2 is necessary to lower olivine

Table 1: Effects of H_2O and CO_2 on olivine liquidus and mantle potential temperature

| P (GPa)	Effect of CO_2			
	a	b	c	d
2	14·00	−0·310	17·65	−0·3213
3	21·35	−0·470	26·76	−0·5819
4	25·34	−0·543	35·1	−0·7949
5	24·60	−0·565	31·65	−0·6745
P (GPa)	Effect of H_2O			
	a	b	c	d
3·5	47·6	−1·185	64·27	−1·671
12·0	86·6	−2·935	109·87	−3·499

a and *b* are parameterizations for olivine liquidus temperature at 1 atm; *c* and *d* are parameterizations for mantle potential temperature.

liquidus temperature and mantle potential temperature for the komatiites.

GEOLOGICAL IMPLICATIONS

Thermal properties of Alexo and Pyke Hill komatiites: a re-evaluation

An important implication of volatile-rich komatiites is that they create ambiguities concerning the thermal properties of the source and all geodynamic interpretations. If we assume that the komatiites from the Abitibi greenstone belt crystallized from a volatile-free primary magma with 30% MgO, the olivine liquidus temperature (i.e. $T_{vf,1}^{OI/L}$) would be 1607 ± 46 °C (Herzberg & Asimow, 2015). Correcting for 0·6% H_2O reported by Sobolev et al. (2016), ignoring the small amount of CO_2 (i.e. 188 ppm), and using the model at 3·5 GPa in Fig. 7a, we calculate $T_{H2O,1}^{OI/L} = 1579 ± 46$ °C; using the method of Falloon & Danyushevsky (2000) to correct for H_2O on liquidus depression, we obtain $T_{H2O,1}^{OI/L} = 1545$ °C. This 1545–1579 °C range is similar to $T_{H2O,1}^{OI/L} = 1532$ °C calculated by Sobolev et al. (2016) using Fe/Mg partitioning from Ford et al. (1983) and corrected for the effects of 0·6% H_2O using the method of Falloon & Danyushevsky (2000). The differences in olivine crystallization temperature can be largely accounted for by the different model effects of 0·6% H_2O; in this study, 0·6% H_2O decreases olivine liquidus temperature by 28 °C, whereas the model of Falloon & Danyushevsky (2000) decreases it by 62 °C. Such differences propagate to mantle potential temperature estimates; these are $TP_{H2O} = 1768$ °C in the present study and 1730 °C estimated by Sobolev et al. (2016), who used equation (5) from Herzberg & Asimow (2015) together with their preferred olivine liquidus temperatures. If the mantle potential temperature of the Archean ambient mantle was in the 1500–1600 °C range (Herzberg et al., 2010), then TP_{H2O} of 1730–1768 °C for the komatiites supports the
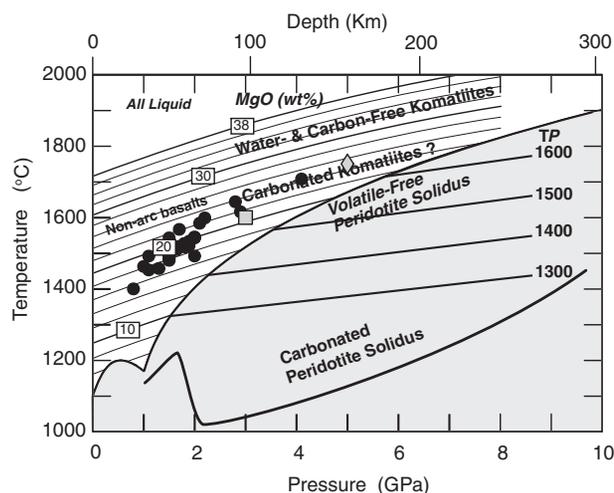
Fig. 8. MgO contents of primary magmas produced by volatile-free melting of peridotite KR4003, and their *T–P* distributions, after Herzberg & Asimow (2015). Lines labeled TP are solid-state adiabatic *T–P* paths. Black filled circles are MgO contents and estimated final *T–P* conditions of melting of Archean and Paleoproterozoic non-arc basalts, given in fig. 5 of Herzberg et al. (2010). Grey filled square and diamond are experimental carbonated komatiite compositions A496 and M354, respectively, with 29% MgO (Dasgupta et al., 2007, 2013; see Figs 5 and 6). Carbonated peridotite solidus is from Dasgupta (2013). The effect of CO_2 is to increase the MgO content of the primary magmas at constant temperature and pressure, relative to volatile-free melting. Most non-arc basalts and carbonated komatiites have MgO contents that are consistent with melting at mantle potential temperatures of 1500–1600 °C.

interpretation that they formed in a mantle plume that was roughly 150 °C hotter (Sobolev et al., 2016). However, as discussed above, this conclusion rests on the assumption that the komatiites with 0·6% H_2O and 30% MgO are primary magmas, and this small water content was sufficient to reduce the SiO_2 content shown in Figs 2 and 3. If instead it is the parental magma that has 0·6% H_2O and 30% MgO, then it may be degassed from the primary magma and the mantle plume interpretation is in doubt, a possibility that is now examined.

In Fig. 8 the MgO contents of model volatile-free primary magmas of peridotite KR4003 and their temperature and pressure distributions (Herzberg & Asimow, 2015) are shown. The MgO isopleths are approximately coincident with the adiabatic decompression *T–P* gradients, and those shown in Fig. 8 are solutions to equations (1) and (2) (Herzberg & Asimow, 2015). Also shown are the temperatures of the 3 and 5 GPa experimental decarbonated melt compositions A496 and M354 (i.e. normalized CO_2-free; Dasgupta et al., 2007, 2013), which have 29% MgO and which I will assume to be primary magma compositions for Alexo and Pyke Hill komatiites. These assumed volatile-generated compositions with 29% MgO share similar *T* and *P* conditions of melting to those that are required to generate volatile-free primary magmas of peridotite KR4003 with

21–25% MgO. Primary magmas produced by deep H_2O- and CO_2-melting of mantle peridotite can have higher MgO contents than those generated by volatile-free melting at similar temperatures and pressures. The *T–P* conditions of melting for the assumed decarbonated primary komatiites A496 and M354 are also similar to those for some primary magmas of the 'non-arc' basalt group of Archean and Paleoproterozoic age (Fig. 8; Herzberg *et al.*, 2010). These basalts formed by partial melting of peridotite with *T*P in the 1500–1600 °C range, conditions that were inferred for the melting of hot ambient mantle, not hot mantle plumes (Herzberg *et al.*, 2010). The similar *T–P* conditions of melting for the assumed decarbonated primary komatiites A496 and M354 indicate that the komatiites might also have formed by melting at ambient mantle temperature conditions.

We can now estimate the volatile contents that the primary magmas must have had to satisfy the condition of melt production in ambient mantle. Using the parameterizations of experimental data in Table 1 and shown in Fig. 7, it is estimated that about 5–6% magmatic CO_2 would be compatible with an ambient mantle *T*P of 1600 °C, in good agreement with the measured CO_2 contents of experiments A496 and M354. About 3% H_2O at 3·5 GPa would also be compatible with ambient mantle melting, but the effects of mixed H_2O–CO_2 contents are not known. Large volatile contents are therefore required for komatiite production in ambient mantle. Future experimental work may falsify these estimates and add strength to the mantle plume model by determining how much H_2O and CO_2 is necessary to satisfy the SiO_2 contents of the Alexo and Pyke Hill komatiites.

If the primary komatiite magma contained 30% MgO and 5% CO_2 then its metastable undegassed olivine liquidus temperature at the surface would be ~1500 °C, about 100 °C lower than the volatile-free condition. This 100 °C variation is similar to the olivine-hosted melt inclusion thermometry of Sobolev *et al.* (2016). Total CO_2 degassing somewhere at depth would trigger about 25% olivine crystallization and drive the MgO content from 30% down to 24%; Mg-numbers of olivine crystals using the Toplis (2005) model at the surface would range from 95·1 to 93·0. This model predicts that lava mobility was sufficient for rapid flow and differentiation, in agreement with field observations and theory (Arndt *et al.*, 2008); it further predicts that not all olivine in komatiite flows grew *in situ*, consistent with chilled margins that contain olivine phenocrysts (Arndt *et al.*, 2008).

Whether the komatiites formed in mantle plumes or ambient mantle, there appears to be no Phanerozoic analogue linking the estimated H_2O and CO_2 contents with trace element contents. In the mantle plume model for which the primary magma contains 0·6% H_2O and 188 ppm CO_2 (Sobolev *et al.*, 2016), H_2O/Ce is 6740 and CO_2/Nb is 700, much higher than for Phanerozoic magmas in which H_2O/Ce is typically 150–300 (Dixon *et al.*, 2002; Saal *et al.*, 2002; Hauri *et al.*, 2006) and CO_2/Nb is

240–540 (Saal *et al.*, 2002; Cartigny *et al.*, 2008). Higher still are ratios for komatiite production under ambient mantle conditions ($H_2O/Ce = 34\,000$ and $CO_2/Nb = 185\,000$ are obtained from 3% H_2O and 5% CO_2). The implication is that water and carbon dioxide are decoupled from trace element abundances in the komatiites owing to delivery in the Transition Zone by early subduction or ingassing during accretion (Sobolev *et al.*, 2016). This decoupling also indicates that primary magma H_2O and CO_2 contents may be high and unconstrained. The ingassing suggestion is examined in more detail below.

Archean tectonics and carbonated wetspots

Uncertainties about primary magma volatile content preclude a unique geodynamic interpretation to be drawn for the Alexo and Pyke Hill komatiites. The mantle plume model for the komatiites will remain secure if the volatile contents measured by Sobolev *et al.* (2016) are actually representative of the primary magma. However, if they represent preservation during olivine crystal growth after extensive degassing, then it is worth examining an alternative to the mantle plume hypothesis. The evidence presented in Fig. 8 suggests that the Alexo and Pyke Hill komatiites may have formed in hot ambient mantle, similar to non-arc basalts. However, the komatiites may have melted much deeper owing to the effects of CO_2 and possibly H_2O in depressing the solidus (Dasgupta, 2013), and unusually deep melting may explain why the komatiites have the geochemical attributes of batch melting (Fig. 1b). The close spatial and temporal association of Alexo and Pyke Hill komatiites with non-arc basalts might indicate that the Archean mantle consisted of compositionally heterogeneous domains that melted at similar ambient mantle temperature conditions (Fig. 8). We can imagine a heterogeneous mantle that consisted of relatively fertile peridotite, which melted to produce the non-arc basalts, and also contained spots, clots or filaments of more depleted and carbonate-bearing hydrous peridotite, which melted to produce the komatiites; these may be 'carbonated wetspots'. Ambient mantle melting for the non-arc basalts (Herzberg *et al.*, 2010) could then be reasonably extended to include the associated komatiites, and it is an alternative to the mantle plume model. It is also distinguished from the formation of Archean komatiites in low-temperature subduction zones (Grove & Parman, 2004). Whatever the correct geodynamic interpretation may be, the komatiites may be recording important degassing events in the Archean.

## Volatile ingassing in the Hadean

It has been proposed that the Hadean Earth had a thick atmosphere of CO_2 and H_2O, and that CO_2 was sequestered by reaction with impact ejecta, oceanic crust, and possibly mantle peridotite to produced carbonates (Sleep & Zahnle, 2001; Sleep *et al.*, 2001; Zahnle *et al.*, 2007). The carbonates were later drawn into the mantle

by some form of subduction. The subduction scenario involves understanding the *T–P* conditions of subducted slabs and carbonate stability and melting. Based on estimates of peak metamorphic conditions for rocks in the Proterozoic and Archean, deep subduction of CO_2 was hindered owing to hotter conditions (Dasgupta & Hirschmann, 2010; Dasgupta, 2013). Thompson *et al.* (2016) concurred by showing that deep mantle ingassing of carbonated oceanic crust is mostly prohibited, even at the present day, because such crust melts in the upper mantle and Transition Zone. The carbonate ingassing problem applies also to water ingassing because hydrous minerals in greenschists and serpentinites have low thermal stabilities (e.g. Schmidt & Poli, 1998). Additionally, although Archean slab temperatures may have been no different from those at present (Syracuse *et al.*, 2010; Palin & White, 2015), extensive dehydration and decarbonation is still expected as slabs heat up during descent into hot ambient mantle. The problem is, how can H_2O and CO_2 be drawn down deep and stored in mantle that is also hot?

The problem of how to ingass the mantle might be resolved if mantle temperatures in the Hadean were lower than those of the Archean (Korenaga, 2008, 2013; Herzberg *et al.*, 2010). However, there is no consensus regarding the final temperature in the Hadean to which the Earth cooled from the thousands of degrees of its initial magma ocean state. Various researchers have suggested complete solidification of the magma ocean within 10^6–10^8 years (Elkins-Tanton, 2008; Hamano *et al.*, 2013; Lupu *et al.*, 2014); the implication is that Hadean mantle potential temperatures would have been cooler than the present-day Earth, and much colder than the Archean Earth (Fig. 9). Other models suggest that the Earth may never have completely solidified (Labrosse *et al.*, 2007; Solomatov, 2015).

Evidence in support of magma ocean solidification within the first 100 Myr is based on a crustal zircon age of 4·37 Ga (Valley *et al.*, 2014). A major caveat is that this 100 Myr time window assumes that the zircons crystallized from some crustal magma that itself was formed by partial melting of a solid peridotite or basalt protolith (e.g. Wilde *et al.*, 2001; Watson & Harrison, 2005; Coogan & Hinton, 2006), not by partial crystallization of the magma ocean. Resolution of the melting versus crystallization problem would identify the end-stage of magma ocean crystallization, and the switchover to partial melting that remained in effect from that point on (Fig. 9).

Pyke Hill komatiites melted from a peridotite source that itself had been partially melted, yielding elevated Sm/Nd (Puchtel *et al.*, 2004, 2009). Puchtel *et al.* (2009) suggested that this initial melting event may have occurred within the first 100 Myr of Earth's history as a result of either global magma ocean differentiation or extraction and subsequent long-term isolation of the early crust. Ingassing of H_2O and CO_2 must have occurred after this initial melting event, not before it. The timing is important because if H_2O and CO_2 were ingassed before the melting event, then it would be
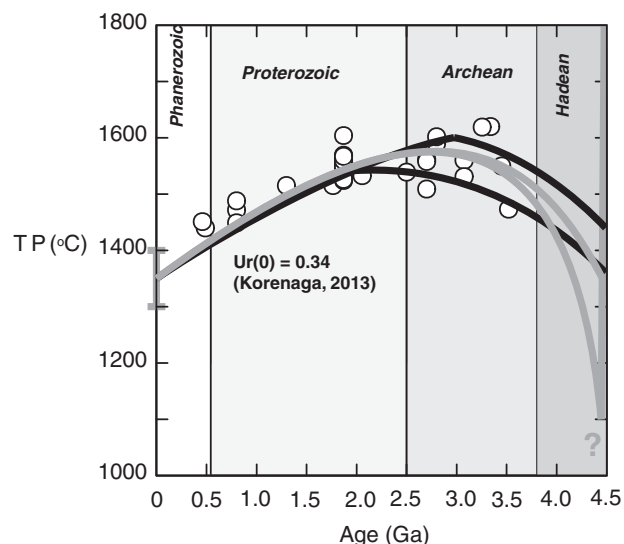
Fig. 9. Models of the thermal history of the Earth. TP is the potential temperature for ambient mantle. White circles are mantle potential temperatures derived by petrological modeling of basalts (Herzberg *et al.*, 2010), modified slightly using PRIMELT3 (Herzberg & Asimow, 2015). Black lines are solutions for stagnant lid and plate-tectonic models, respectively (Korenaga, 2013); Ur(0), present-day Urey ratio. Grey lines demonstrate the switchover from magma ocean cooling and crystallization to mantle heating by radioactive decay in the Hadean; they are roughly constrained by the petrological models and the need to ingas carbonate in the Hadean by subduction (Dasgupta, 2013). There is great uncertainty in mantle potential temperature during the Hadean. Fully crystallized magma ocean models (Elkins-Tanton, 2008; Hamano *et al.*, 2013; Lupu *et al.*, 2014) are defined by absolute and mantle potential temperatures that must be below the peridotite solidus temperature at the surface (1100°C; Hirschmann, 2000; Herzberg & Asimow, 2015), but more work is needed to evaluate this possibility (Solomatov, 2015).

difficult to understand how melting did not drive off H_2O and CO_2. Also, ingassing after the melting event by subduction would affect other highly incompatible lithophile trace elements, which is not observed (Sobolev *et al.*, 2016).

Although the thermal history of the Earth within the first 100 Myr is an unresolved and defining issue, the evidence presented above for volatiles in Archean komatiites indicates that parts of the deep Earth may have been sufficiently cool at some point in the Hadean to ingas the mantle with H_2O and CO_2. Flipping this around, it is difficult to imagine how the mantle could have ingassed H_2O and CO_2 and preserved the ^{142}Nd, ^{129}Xe, and ^{182}W isotopic compositions of short-lived radionuclides (Willbold *et al.*, 2011, 2015; Mukhopadhyay, 2012; Rizo *et al.*, 2012, 2016; Touboul *et al.*, 2012, 2014; Puchtel *et al.*, 2016) in a hot, extensively melted, long-lived, and well-mixed Hadean mantle.

Volcanic outgassing and the Great Oxidation Event

The Archean atmosphere consisted mostly of CO_2 and CH_4, greenhouse gases that prevented the Earth's surface from freezing owing to the lower solar luminosity

(Walker, 1977; Kasting, 1993; Pavlov *et al.*, 2000). The evidence presented in this study and by Sobolev *et al.* (2016) for CO_2 and H_2O outgassing in komatiites supports prior models of the Archean atmosphere that reasonably assumed a volcanic provenance to atmospheric CO_2 (e.g. Kasting, 1993). However, it is likely that methanogenic archaea contributed the bulk of atmospheric CH_4 (Walker, 1977; Pavlov *et al.*, 2000; Konhauser *et al.* 2009) through the metabolic reaction

$$CO_2 + 4H_2 \rightarrow CH_4 + 2H_2O. \qquad (11)$$
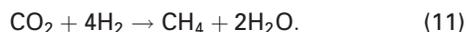
In contrast, atmospheric oxygen can be produced from oxygenic photosynthetic cyanobacteria as represented by the reaction

$$CO_2 + H_2O \rightarrow CH_2O + O_2. \qquad (12)$$

The instability of oxygen and methane can be represented with the reactions (Daines & Lenton, 2016)

$$CH_4 + 2O_2 \rightarrow CO_2 + H_2O \qquad (13)$$

and

$$CH_4 + CO_2 + O_2 \rightarrow 2CO_2 + H_2. \qquad (14)$$

Given reactions (13) and (14), we may ask: did the rise of atmospheric O_2 lead to the demise of CH_4 (Pavlov *et al.*, 2000; Zahnle *et al.*, 2006)? Or was it the reduction in atmospheric CH_4 that led to the rise of O_2 and the Great Oxidation Event at around 2·4 Ga (Konhauser *et al.*, 2009)?

Konhauser *et al.* (2009) suggested that the decrease in biogenic methane production was related to the drop in Ni/Fe in banded iron formations, and inferred that this reflected a reduction in dissolved Ni in seawater (see also Kamber, 2010). Nickel is an important metal in several enzymes that catalyze methanogenesis (Jaun & Thauer, 2007), and Konhauser *et al.* (2009) proposed that the decline of nickel in the oceans could have stifled the activity of archaea and disrupted the supply of biogenic methane. They further proposed that the decline in dissolved oceanic Ni was related to the decline in the eruption of Ni-rich volcanic rocks, which were the source of dissolved oceanic nickel.

It is well known that komatiites are predominantly Archean in age. The few komatiites that have erupted in the Phanerozoic differ in having lower MgO contents, and they contain olivine with lower Mg numbers (e.g. Herzberg *et al.* 2007; Arndt *et al.*, 2008; Herzberg & Gazel, 2009). Furthermore, the Ni content of any peridotite-source primary magma is positively related to its primary magma MgO content (Herzberg, 2011). Arndt (1991) concluded that Archean basalts were elevated in Ni compared with modern lavas. However, secular trends can be complicated owing to fractional crystallization of olivine, yielding a wide range of Ni-rich olivine cumulates and Ni-poor derivative liquids. Calculated Ni contents of primary magmas eliminate this noise; results are shown in Fig. 10 together with secular changes in the model time-averaged Ni content
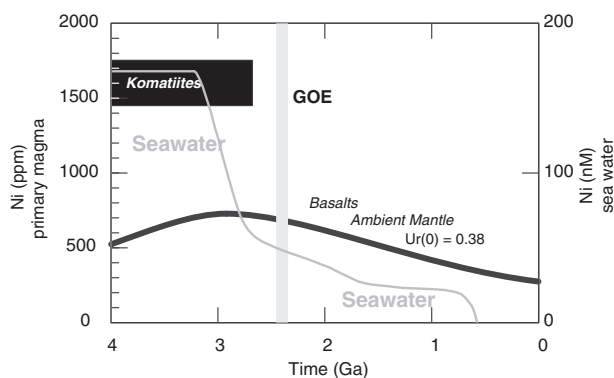
Fig. 10. The Ni contents of seawater and the primary magmas of basalts and komatiites. The seawater curve represents the calculated average dissolved Ni from the time-averaged Ni/Fe of banded iron formations (Konhauser *et al.*, 2009). The black curve represents calculated Ni contents of primary basaltic magmas from ambient mantle with a present-day Urey ratio of 0·38, calculated from the MgO contents given by Herzberg *et al.* (2010) and the relationship Ni (ppm) $= 21·6$MgO $- 0·32$MgO$^2 + 0·051$MgO^3 (Herzberg, 2011), which is appropriate for MgO $< 27\%$. Ni contents of komatiites are those for batch and accumulated fractional melting of a peridotite source KR4003; with MgO $= 30\%$ a $\pm 4\%$ uncertainty in primary magma MgO propagates to ± 370 ppm Ni. GOE, Great Oxidation Event.

of seawater (Konhauser *et al.*, 2009). For all Archean komatiites, I assume 30% MgO in the primary magma, although a range of 26–34% (Robin-Popieul *et al.*, 2012) covers all possibilities. A primary magma with 30% MgO will contain 1440 ppm Ni if it formed by batch melting of fertile peridotite similar to KR4003, and 1760 ppm if formed by accumulated fractional melting (Fig. 10; Herzberg, 2011). Although komatiites are the most Ni-rich volcanic rocks on Earth, basalts produced by melting ambient mantle have much lower Ni contents. The basalt Ni contents shown in Fig. 10 are appropriate for MgO contents of primary basaltic magmas that melted from ambient mantle having a present-day Urey ratio of 0·38 (Herzberg *et al.*, 2010). What is clear from Fig. 10 is that the dissolved Ni content of seawater was at a maximum during Ni-rich komatiite production in the Archean.

Komatiites are abundant in the Abitibi greenstone belt, absent in other Archean greenstone belts and, on average, constitute less than 5% of the volcanic rocks (de Wit & Ashwal, 1997). Evidence from Ni/Co and Cr/Zn in Archean terrigenous sedimentary rocks indicates a time progressive reduction in the amount of komatiite eroded during the Archean (Tang *et al.*, 2016). And the correlation between Ni-rich komatiite production and maximum dissolved Ni in seawater (Fig. 10) is evidence that supports the hypothesis of Konhauser *et al.* (2009) that there was a nickel famine at the end of the Archaean owing to a shutdown of komatiite volcanism; it further supports their idea that this caused a collapse of biogenic methane production, which facilitated the rise of atmospheric oxygen. It is difficult to improve on the quote from Konhauser *et al.* (2009) that 'the

enzymatic reliance of methanogens on a diminishing supply of volcanic nickel links mantle evolution to the redox state of the atmosphere'. Those researchers attributed the end-Archean drop in komatiite production and eruption to a decrease in hot mantle plume activity (Barley *et al.*, 1998; Konhauser *et al.*, 2009). However, this interpretation now rests on significant uncertainty about how H_2O and CO_2 have compromised our ability to constrain mantle temperature. It is worth entertaining the conjecture that the shutdown in komatiite production followed the purging of a substantial volatile-rich reservoir in the mantle during a great komatiite 'belching' event.

DISCUSSION AND CONCLUSIONS

Komatiites from Alexo and Pyke Hill in the Archean Abitibi greenstone belt provide petrological evidence for an early Earth carbon and water cycle, ingassing in the cool Hadean and outgassing in the hot Archean. The komatiites have SiO_2 contents that are lower than those expected of advanced volatile-free melting of mantle peridotite. The SiO_2 misfit cannot be plausibly accounted for by variations in model Bulk Earth peridotite composition, a source that had experienced a prior stage of perovskite fractionation in a magma ocean, addition of chondrites, or a source that had recycled crust added to it. Serpentinization is also not a plausible explanation because it results in SiO_2 gain, not SiO_2 loss (Malvoisin, 2015). One possible resolution to the silica misfit problem is obtained if the komatiites from Alexo and Pyke Hill were generated from carbonated peridotite, a conclusion based on the reasonable agreement between komatiite major elements (i.e. SiO_2, Al_2O_3, FeO, MgO, and CaO) and those of experiments by Dasgupta *et al.* (2007, 2103) using a carbonated peridotite composition. High-degree melts with olivine as the sole residual phase can have low SiO_2 contents owing to carbonate addition. Furthermore, a role for significant H_2O is indicated from recent melt inclusion studies (Sobolev *et al.*, 2016).

Abitibi komatiite melt inclusion ratios of H_2O/Ce and CO_2/Nb (Sobolev *et al.*, 2016) are much higher than those in Phanerozoic ocean island basalts. The decoupling of volatiles and lithophile trace elements indicates that primary magma H_2O and CO_2 contents may be high and difficult to constrain. It is not clear if the elevated H_2O and CO_2 contents are those in the parental magma at the time of olivine crystallization or in the primary magma from the mantle. If degassing was extensive, the volatile contents plausibly represent minimum bounds on the CO_2 and H_2O contents of the primary magmas from the mantle source. The SiO_2 contents and perhaps other major elements of komatiites may preserve the memory of primary magma volatile content that is otherwise lost to degassing. More work is needed to constrain how much CO_2 and H_2O is required to resolve the SiO_2 misfit, and the *T–P* conditions of melting. Failure to do so imposes significant uncertainty

about Archean mantle potential temperature and geodynamic interpretations. These uncertainties notwithstanding, the komatiites appear to be recording important degassing events in the Archean.

The conclusion about a carbonated and hydrous peridotite source for Alexo and Pyke Hill cannot be reliably generalized to other Archean komatiites; each komatiite occurrence may have its own unique volatile content, and the problem must be examined on a case-by-case basis. However, attention is drawn to komatiites from the Belingwe greenstone belt in Zimbabwe, which have spinel-hosted melt inclusions that contain 1·1% H_2O and 17·5% MgO, as noted by Shimizu *et al.* (2001). Those researchers recognized that the H_2O content of the melt inclusions may represent minimum bounds owing to degassing of the primary magma. Uncertainties in volatile content arising from degassing impose significant uncertainty about Archean mantle potential temperature and geodynamic interpretations. Hydrous and CO_2-rich komatiites could have formed from 'carbonated wetspots' in mantle plumes or ambient mantle, and more work is needed to constrain the problem.

The Alexo–Pyke Hill komatiites of Archean age provide evidence for an early Earth carbon and water cycle. Ingassing may have occurred in the Hadean when atmospheric CO_2 and H_2O was sequestered by reaction with impact ejecta, oceanic crust, and mantle peridotite to produced carbonates and hydrous minerals (Sleep & Zahnle, 2001; Sleep *et al.*, 2001; Zahnle *et al.*, 2007). A major problem involves understanding the kinds of tectonic processes that drew and stored carbonates and hydrous phases deep into the Earth's interior. A possible solution to the problem is obtained if parts of the Earth's deep mantle were sufficiently cool at some point in the Hadean (Fig. 9) to ingas it with carbonate and hydrous minerals. This idea is consistent with a variety of constraints from zircon studies (Valley *et al.*, 2002; Watson & Harrison, 2005; Coogan & Hinton, 2006; Hopkins *et al.*, 2008; Bell *et al.*, 2015), and the need to preserve ^{142}Nd, ^{129}Xe, and ^{182}W isotopic anomalies in rocks of various ages (Willbold *et al.*, 2011, 2015; Mukhopadhyay, 2012; Rizo *et al.*, 2012, 2016; Touboul *et al.*, 2012, 2014; Puchtel *et al.*, 2016). Cold Hadean ingassing was followed by hot Archean outgassing associated with komatiite production in ambient mantle or mantle plumes.

The substantial decline of komatiite eruptions after ~2·7 Ga has been attributed to the termination of a global plume-breakout event (Barley *et al.*, 1998; Konhauser *et al.*, 2009). However, this interpretation now rests on uncertainty about how H_2O and CO_2 have compromised our ability to constrain mantle temperature and geodynamic setting. It is worth entertaining the conjecture that widespread komatiite production at 2·7 Ga was a consequence of the outgassing of a substantial volatile-rich mantle reservoir. Once purged, komatiite volcanism shut down. As komatiites are the most nickel-rich volcanic rocks on Earth, the

termination of their eruption could have caused a nickel famine in Archean oceans, and a collapse of biogenic methane production, which facilitated the rise of atmospheric oxygen (Konhauser *et al.*, 2009). Komatiites may have played a significant role in Archean atmosphere and biological evolution.

REFERENCES

Agee, C. B. (1998). Crystal–liquid density inversions in terrestrial and lunar magmas. *Physics of the Earth and Planetary Interiors* **107**, 63–74.

Allègre, C. J., Poirier, J.-P., Humler, E. & Hofmann, A. W. (1995). The chemical composition of the Earth. *Earth and Planetary Science Letters* **134**, 515–526.

Arndt, N. T. (1986). Differentiation of komatiites flows. *Journal of Petrology* **27**, 279–301.

Arndt, N. T. (1991). High Ni in Archean tholeiites. *Tectonophysics* **187**, 411–420.

Arndt, N. T. (2003). Komatiites, kimberlites, and boninites. *Journal of Geophysical Research* **108**, 2293.

Arndt, N. T., Lesher, C. M. & Barnes, S. J. (2008). *Komatiite*. Cambridge University Press, 467 pp.

Arth, J. G., Arndt, N. T. & Naldrett, A. J. (1977). Genesis of Archean komatiite from Munro Township, Ontario: trace element evidence. *Geology* **5**, 590–594.

Barley, M. E., Krapez, B., Groves, D. I. & Kerrich, R. (1998). The Late Archean bonanza: metallogenic and environmental consequences of the interaction between mantle plumes, lithospheric tectonics and global cyclicity. *Precambrian Research* **91**, 65–90.

Bell, E. A., Boehnke, P., Harrison, T. M. & Mao, W. L. (2015). Potentially biogenic carbon preserved in a 4·1 billion-year-old zircon. Proceedings of the National Academy of Sciences *of the USA*. doi:10.1073/pnas.1517557112.

Berry, A. J., Danyushevsky, L. V., O'Neill, H. St. C., Newville, M. & Sutton, S. R. (2008). Oxidation state of iron in komatiite melt inclusions indicates hot Archaean mantle. *Nature* **455**, 960–963.

Bickle, M. J. (1982). The magnesium contents of komatiitic liquids. In: Arndt, N. T. & Nisbet, E. G. (eds) *Komatiites*. George Allen & Unwin, pp. 479–494.

Blichert-Toft, J. & Puchtel, I. S. (2010). Depleted mantle sources through time: Evidence from Lu–Hf and Sm–Nd isotope systematics of Archean komatiites. *Earth and Planetary Science Letters* **297**, 598–606.

Campbell, I., Griffiths, R. W. & Hill, R. I. (1989). Melting in an Archaean mantle plume: heads it's basalts, tails it's komatiites. *Nature* **339**, 697–699.

Canil, D. (1997). Vanadium partitioning and the oxidation state of Archaean komatiite magmas. *Nature* **389**, 842–845.

Cartigny, P., Pineau, F., Aubaud, C. & Javoy, M. (2008). Towards a consistent mantle carbon flux estimate: Insights from volatile systematics (H_2O/Ce, dD, CO_2/Nb) in the North Atlantic mantle (14°N and 34°N). *Earth and Planetary Science Letters* **265**, 672–685.

Coogan, L. A. & Hinton, R. W. (2006). Do the trace element compositions of detrital zircons require Hadean continental crust? *Geology* **34**, 633–636.

Daines, S. J. & Lenton, T. M. (2016). The effect of widespread early aerobic marine ecosystems on methane cycling and the Great Oxidation. *Earth and Planetary Science Letters* **434**, 42–51.

Dasgupta, R. (2013). Ingassing, storage, and outgassing of terrestrial carbon through geologic time. In: Hazen, R. M., Jones, A. P. & Baross, J. A. (eds) *Carbon in Earth. Mineralogical Society of America and Geochemical Society, Reviews in Mineralogy and Geochemistry* **75**, 183–229.

Dasgupta, R. & Hirschmann, M. M. (2010). The deep carbon cycle and melting in Earth's interior. *Earth and Planetary Science Letters* **298**, 1–13.

Dasgupta, R., Hirschmann, M. M. & Smith, N. D. (2007). Partial melting experiments on peridotite + CO_2 at 3 GPa and genesis of alkalic ocean island basalts. *Journal of Petrology* **48**, 2093–2124.

Dasgupta, R., Mallik, A., Tsuno, K., Withers, A. C., Hirth, G. & Hirschmann, M. M. (2013). Carbon-dioxide-rich silicate melt in the Earth's upper mantle. *Nature* **493**, 211–215.

Davis, F. A., Tangeman, J. A., Tenner, T. J. & Hirschmann, M. M. (2009). The composition of KLB-1 peridotite. *American Mineralogist* **94**, 176–180.

de Wit, M. J. & Ashwal, L. D. (1997). Convergence towards divergent models of greenstone belts. In: de Wit, M. & Ashwal, L. D. (eds) *Greenstone Belts, Oxford Monograph on Geology and Geophysics*, **35**. Oxford University Press, pp. ix–xvii.

Dixon, J. E., Leist, L., Langmuir, C. & Schilling, J.-G. (2002). Recycled dehydrated lithosphere observed in plume-influenced mid-ocean-ridge basalt. *Nature* **420**, 385–389.

Elkins-Tanton, L. T. (2008). Linked magma ocean solidification and atmospheric growth for Earth and Mars. *Earth and Planetary Science Letters* **271**, 181–191.

Falloon, T. J. & Danyushevsky, L. V. (2000). Melting of refractory mantle at 1·5, 2 and 2·5 GPa under anhydrous and H_2O-undersaturated conditions: implications for the petrogenesis of high-Ca boninites and the influence of subduction components on mantle melting. *Journal of Petrology* **41**, 257–283.

Fan, J. & Kerrich, R. (1997). Geochemical characteristics of aluminum depleted and undepleted komatiites and HREE-enriched low-Ti tholeiites, Western Abitibi greenstone belt: a heterogeneous mantle plume-convergent margin environment. *Geochimica et Cosmochimica Acta* **61**, 4723–4744.

Ford, C. E., Russell, D. G., Craven, J. A. & Fisk, M. R. (1983). Olivine–liquid equilibria: temperature, pressure and composition dependence of the crystal/liquid cation partition coefficients for Mg, Fe^{2+}, Ca and Mn. *Journal of Petrology* **24**, 256–265.

Grove, T. L. & Parman, S. W. (2004). Thermal evolution of the Earth as recorded by komatiites. *Earth and Planetary Science Letters* **219**, 173–187.

Hamano, K., Abe, Y. & Genda, H. (2013). Emergence of two types of terrestrial planet on solidification of magma ocean. *Nature* **497**, 607–610.

Hart, S. R. & Zindler, A. (1986). In search of a bulk-Earth composition. *Chemical Geology* **57**, 247–267.

Hauri, E. H., Gaetani, G. A. & Green, T. H. (2006). Partitioning of water during melting of the Earth's upper mantle at H_2O-undersaturated conditions. *Earth and Planetary Science Letters* **248**, 715–734.

Herzberg, C. T. (1992). Depth and degree of melting of komatiites. *Journal of Geophysical Research* **97**, 4521–4540.

Herzberg, C. T. (1993). Lithosphere peridotites of the Kaapvaal craton. *Earth and Planetary Science Letters* **120**, 13–29.

Herzberg, C. (2004). Geodynamic information in peridotite petrology. *Journal of Petrology* **45**, 2507–2530.

Herzberg, C. (2011). Identification of source lithology in the Hawaiian and Canary Islands: implications for origins. *Journal of Petrology* **52**, 113–146.

Herzberg, C. & Asimow, P. D. (2015). PRIMELT3 MEGA.XLSM software for primary magma calculation: peridotite primary magma MgO contents from the liquidus to the solidus. *Geochemistry, Geophysics, Geosystems* **16**, 563–578.

Herzberg, C. & Gazel, E. (2009). Petrological evidence for secular cooling in mantle plumes. *Nature* **458**, 619–622.

Herzberg, C. T. & O'Hara, M. J. (1985). Origin of mantle peridotite and komatiite by partial melting. *Geophysical Research Letters* **12**, 541–544.

Herzberg, C. & O'Hara, M. J. (2002). Plume-associated ultramafic magmas of Phanerozoic age. *Journal of Petrology* **43**, 1857–1883.

Herzberg, C., Asimow, P. D., Arndt, N., Niu, Y., Lesher, C. M., Fitton, J. G., Cheadle, M. J. & Saunders, A. D. (2007). Temperatures in ambient mantle and plumes: constraints from basalts, picrites and komatiites. *Geochemistry, Geophysics, Geosystems* **8**, Q02006.

Herzberg, C., Condie, K. & Korenaga, J. (2010). Thermal history of the Earth and its petrological expression. *Earth and Planetary Science Letters* **292**, 79–88.

Hirschmann, M. M. (2000). Mantle solidus: Experimental constraints and the effects of peridotite composition. *Geochemistry, Geophysics, Geosystems* **1**, doi:10.1029/2000GC000070.

Hopkins, M., Harrison, C. E. & Manning, C. E. (2008). Low heat flow inferred from >4 Gyr zircons suggests Hadean plate boundary interactions. *Nature* **456**, 493–496.

Jackson, M. G. & Jellinek, A. M. (2013). Major and trace element composition of the high $^3He/^4He$ mantle: implications for the composition of a nonchondritic Earth. *Geochemistry, Geophysics, Geosystems* **14**, 2954–2976.

Jagoutz, E., Palme, H., Baddenhausen, H., Blum, K., Cendales, M., Dreibus, G., Spettel, B., Lorenz, V. & Wanke, H. (1979). The abundances of major, minor and trace elements in the Earth's mantle as derived from primitive ultramafic nodules. *Proceedings of the 10th Lunar and Planetary Science Conference. Geochimica et Cosmochimica Acta Supplement* **10**, 2031–2050.

Jarvis, G. T. & Campbell, I. H. (1983). Archean komatiites and geotherms: solution to an apparent contradiction. *Geophysical Research Letters* **10**, 1133–1136.

Jaun, B. & Thauer, R. K. (2007). Methyl-coenzyme M reductase and its nickel corphin coenzyme F_{430} in methanogenic archaea. In: Sigel, A., Sigel, H. & Sigel, R. K. O. (eds) *Nickel and its Surprising Impact in Nature. Metal Ions in Life Sciences, 2.* Wiley, pp. 323–356.

Kamber, B. S. (2010). Archean mafic-ultramafic volcanic landmasses and their effect on ocean-atmosphere chemistry. *Chemical Geology* **274**, 19–28.

Kasting, J. F. (1993). Earth's early atmosphere. *Science* **259**, 920–926.

Kawamoto, T. & Holloway, J. R. (1997). Melting temperature and partial melt chemistry of H_2O-saturated mantle peridotite to 11 gigapascals. *Science* **276**, 240–243.

Konhauser, K. O., Pecoits, E., Lalonde, S. V., Papineau, D., Nisbet E. G., Barley, M. E., Arndt, N. T., Zahnle, D. & Kamber, B. S. (2009). Oceanic nickel depletion and a methanogen famine before the Great Oxidation Event. *Nature* **458**, 750–753.

Korenaga, J. (2008). Urey ratio and the structure and evolution of Earth's mantle. *Reviews of Geophysics* **46**, RG2007.

Korenaga, J. (2013). Initiation and evolution of plate tectonics on Earth: theories and observations. *Annual Review of Earth and Planetary Sciences* **41**, 117–151.

Labrosse, S., Hernlund, J. W. & Coltice, N. (2007). A crystallizing dense magma ocean at the base of the Earth's mantle. *Nature* **450**, 866–869.

Lahaye, Y. & Arndt, N. T. (1996). Alteration of a komatiitic flow: Alexo, Ontario, Canada. *Journal of Petrology* **37**, 1261–1284.

Lahaye, Y., Arndt, N. T., Byerly, G., Chauvel, C., Fourcade, S. & Gruau, G. (1995). The influence of alteration on the trace-element and Nd-isotopic compositions of komatiites. *Chemical Geology* **126**, 43–64.

Langmuir, C. H., Klein, E. M. & Plank, T. (1992). Petrological systematics of Mid-Ocean Ridge Basalts: constraints on melt generation beneath ocean ridges. In: Morgan, J. P., Blackman, D. K. & Sinton, J. M. (eds) *Mantle Flow and Melt Generation at Mid-Ocean Ridges.* American Geophysical Union, Geophysical Monograph **71**, 183–280.

Lupu, R. E., Zahnle, K., Marley, M. S., Schaefer, L., Fegley, B., Morley, C., Cahoy, K., Freedman, R. & Fortney, J. J. (2014). The atmospheres of Earthlike planets after giant impact events. *Astronomical Journal* **784**, doi:10.1088/0004-637X/784/1/27.

Lyubetskya, T. & Korenaga, J. (2007). Chemical composition of Earth's primitive mantle and its variance: 1. Methods and results. *Journal of Geophysical Research* **112**, B03211.

Malvoisin, B. (2015). Mass transfer in the oceanic lithosphere: serpentinization is not isochemical. *Earth and Planetary Science Letters* **430**, 75–85.

McDonough, W. F. & Sun, S.-s. (1995). The composition of the Earth. *Chemical Geology* **120**, 223–253.

Mukhopadhyay, S. (2012). Early differentiation and volatile accretion recorded in deep-mantle neon and xenon. *Nature* **486**, 101–104.

Nisbet, E. G., Cheadle, M. J., Arndt, N. T. & Bickle, M. J. (1993). Constraining the potential temperature of the Archaean mantle: review of the evidence from komatiites. *Lithos* **30**, 291–307.

O'Hara, M. J. (1965). Primary magmas and the origin of basalts. *Scottish Journal of Geology* **1**, 19–40.

Ohtani, E. (1985). The primordial terrestrial magma ocean and its implication for stratification of the mantle. *Physics of the Earth and Planetary Interiors* **38**, 70–80.

Ohtani, E., Suzuki, A. & Kato, T. (1998). Flotation of olivine and diamond in mantle melt at high pressure: Implications for fractionation in the deep mantle and ultradeep origin of diamond. In: Manghnani, M. H. & Yagi, T. (eds) *Properties of Earth and Planetary Materials. American Geophysical Union, Geophysical Monograph* **101**, 227–239.

Palin, R. M. & White, R. W. (2015). Emergence of blueschists on Earth linked to secular changes in oceanic crust composition. *Nature Geoscience*. doi:10.1038/NGEO2605.

Palme, H. & O'Neill, H. S. C. (2003). Cosmochemical estimates of mantle composition. In: Carlson, R. W., Holland, H. D. & Turekian, K. K. (eds) *Treatise on Geochemistry, 2, The Mantle and Core*. Elsevier, pp. 1–38.

Parman, S. W. & Grove, T. L. (2004). Harzburgite melting with and without H_2O: experimental data and predictive modeling. *Journal of Geophysical Research* **109**, B02201.

Parman, S. W., Dann, J. C., Grove, T. L. & de Wit, M. J. (1997). Emplacement conditions of komatiite magmas from the 3·49

Ga Komati Formation, Barberton Greenstone Belt, South Africa. *Earth and Planetary Science Letters* **150**, 303–323.

Pavlov, A. A., Kasting, J. F., Brown, L. L., Rages, K. A. & Freedman, R. (2000). Greenhouse warming by CH_4 in the atmosphere of early Earth. *Journal of Geophysical Research* **105**, 11981–11990.

Puchtel, I. S., Humayun, M., Campbell, A. J., Sproule, R. A., & Lesher, C. M. (2004). Platinum group element geochemistry of komatiites from the Alexo and Pyke Hill areas, Ontario, Canada. *Geochimica et Cosmochimica Acta* **68**, 1361–1383.

Puchtel, I. S., Walker, R. J., Brandon, A. D. & Nisbet, E. G. (2009). Pt–Re–Os and Sm–Nd isotope and HSE and REE systematics of the 2·7 Ga Belingwe and Abitibi komatiites. *Geochimica et Cosmochimica Acta* **73**, 6367–6389.

Puchtel, I. S., Blichert-Toft, J., Touboul, M., Walker, R. J., Byerly, G. R., Nisbet, E. G. & Anhaeusser, C. R. (2013). Insights into early Earth from Barberton komatiites: evidence from lithophile isotope and trace element systematics. *Geochimica et Cosmochimica Acta* **108**, 63–90.

Puchtel, I. S., Blichert-Toft, J., Touboul, M., Horan M. F., Walker, R. J. (2016). The coupled [182]W–[142]Nd record of early terrestrial mantle differentiation. *Geochemistry, Geophysics, Geosystems* **17**, 2168–2193.

Putirka, K. D. (2008). Thermometers and barometers for volcanic systems. In: Putirka, K. D. & Tepley, F. J., III (eds) *Minerals, Inclusions and Volcanic Processes. Mineralogical Society of America and Geochemical Society, Reviews in Mineralogy and Geochemistry* **69**, 61–120.

Putirka, K. D., Perfit, M., Ryerson, F. J. & Jackson, M. G. (2007). Ambient and excess mantle temperatures, olivine thermometry, and active vs. passive upwelling. *Chemical Geology* **241**, 177–206.

Ringwood, A. E. (1979). *Origin of the Earth and Moon*. Springer, 295 pp.

Rizo, H., Boyet, M., Blichert-Toft, J., O'Neil, J., Rosing, M. T. & Paquette, J.-L. (2012). The elusive Hadean enriched reservoir revealed by [142]Nd deficits in Isua Archaean rocks. *Nature* **491**, 96–100.

Rizo, H., Walker, R. J., Carlson, R. W., Horan, M. F., Mukhopadhyay, S., Manthos, V., Francis, D. & Jackson, M. G. (2016). Preservation of Earth-forming events in the tungsten isotopic composition of modern flood basalts. *Science* **352**, 809–812.

Robin-Popieul, C. C. M., Arndt, N. T., Chauvel, C., Byerly, G. R., Sobolev, A. V. & Wilson, A. (2012). A new model for Barberton komatiites: deep critical melting with high melt retention. *Journal of Petrology* **53**, 2191–2229.

Saal, A. E., Hauri, E. H., Langmuir, C. H. & Perfit, M. R. (2002). Vapour undersaturation in primitive mid-ocean-ridge basalt and the volatile content of Earth's upper mantle. *Nature* **419**, 451–455.

Schmidt, M. W. & Poli, S. (1998). Experimentally based water budgets for dehydrating slabs and consequences for arc magma generation. *Earth and Planetary Science Letters* **163**, 361–379.

Shimizu, K., Komiya, T., Hirose, K., Shimizu, N. & Maruyama, S. (2001). Cr-spinel, an excellent micro-container for retaining primitive melts—implications for a hydrous plume origin for komatiites. *Earth and Planetary Science Letters* **189**, 177–188.

Shore, M. (1996). Cooling and crystallization of komatiite flows. PhD thesis, University of Ottawa.

Sleep, N. H. & Zahnle, K. (2001). Carbon dioxide cycling and implications for climate on ancient Earth. *Journal of Geophysical Research* **106**, 1373–1399.

Sleep, N. H., Zahnle, K. & Neuhoff, P. S. (2001). Initiation of clement surface conditions on the earliest Earth. *Proceedings of the National Academy of Sciences of the USA* **98**, 3666–3672.

Sobolev, A. V., Hofmann, A. W., Kuzmin, D. V., Yaxley, G. M., Arndt, N. T., Chung, S.-L., Danyushevsky, L. V., Elliott, T., Frey, F. A., Garcia, M. O., Gurenko, A. A., Kamenetsky, V. S., Kerr, A. C., Krivolutskaya, N. A., Matvienkov, V. V., Nikogosian, I. K., Rocholl, A., Sigurdsson, I. A., Sushchevskaya, N. M. & Teklay M. (2007). The amount of recycled crust in sources of mantle-derived melts. *Science* **316**, 412–417.

Sobolev, A. V., Asafov, E. V., Gurenko, A. A., Arndt, N. T., Batanova, V. G., Portnyagin, M. V., Garbe-Schönberg, D. & Krasheninnikov, S. P. (2016). Komatiites reveal an Archean hydrous deep-mantle reservoir. *Nature* **531**, 628–632.

Solomatov, V. (2015). Magma oceans and primordial mantle differentiation. In: Shubert, G. (ed.) *Treatise on Geophysics*, **9**, 2nd edn, Elsevier, Amsterdam, pp. 81–104.

Sproule, R. A., Lesher, C. M., Ayer, J. A., Thurston, P. C. & Herzberg, C. T. (2002). Spatial and temporal variations in the geochemistry of komatiites and komaiitic basalts in the Abitibi greenstone belt. *Precambrian Research* **115**, 153–186.

Sugawara, T. (2000). Empirical relationships between temperature, pressure, and MgO content in olivine and pyroxene saturated liquid. *Journal of Geophysical Research* **105**, 8457–8472.

Syracuse, E. M., van Keken, P. E. & Abers, G. A. (2010). The global range of subduction zone thermal models. *Physics of the Earth and Planetary Interiors* **183**, 73–90.

Tang, M., Chen, K. & Rudnick, R. L. (2016). Archean upper crust transition from mafic to felsic marks the onset of plate tectonics. *Science* **351**, 372–375.

Tenner, T. J., Hirschmann, M. M. & Munir, H. (2012a). The effect of H_2O on partial melting of garnet peridotite at 3·5 GPa. *Geochemistry, Geophysics, Geosystems* **13**, Q03016.

Tenner, T. J., Hirschmann, M. M., Withers, A. C. & Ardia, P. (2012b). H_2O storage capacity of olivine and low-Ca pyroxene from 10 to 13 GPa: consequences for dehydration melting above the transition zone. *Contributions to Mineralogy and Petrology* **163**, 297–316.

Thompson, A. R., Walter, M. J., Kohn, S. C. & Brooker, R. A. (2016). Slab melting as a barrier to deep carbon subduction. *Nature* **529**, 76–79.

Toplis, M. J. (2005). The thermodynamics of iron and magnesium partitioning between olivine and liquid: criteria for assessing and predicting equilibrium in natural and experimental systems. *Contributions to Mineralogy and Petrology* **149**, 22–39.

Touboul, M., Puchtel, I. S. & Walker, R. J. (2012). [182]W evidence for long-term preservation of early mantle differentiation products. *Science* **335**, 1065–1069.

Touboul, M., Liu, J., O'Neil, J., Puchtel, I. S. & Walker, R. J. (2014). New insights into the Hadean mantle revealed by [182]W and highly siderophile element abundances of supracrustal rocks from the Nuvvuagittuq Greenstone Belt, Quebec, Canada. *Chemical Geology* **383**, 63–75.

Trønnes, R. G. & Frost, D. J. (2002). Peridotite melting and mineral–melt partitioning of major and minor elements at 22–24·5 GPa. *Earth and Planetary Science Letters* **197**, 117–131.

Valley, J. W., Peck, W. H., King, E. M. & Wilde, S. A. (2002). A cool early Earth. *Geology* **30**, 351–354.

Valley, J. W., Cavosie, A. J., Ushikubo, T., Reinhard, D. A., Lawrence, D. F., Larson, D. J., Clifton, P. H., Kelly, T. F., Wilde, S. A., Moser, D. E. & Spicuzza, M. J. (2014). Hadean age for a post-magma-ocean zircon confirmed by atom-probe tomography. *Nature Geoscience* **7**, 219–223.

Walker, J. C. G. (1977). *Evolution of the Atmosphere*. Macmillan, 318 pp.

Walter, M. J. (1998). Melting of garnet peridotite and the origin of komatiite and depleted lithosphere. *Journal of Petrology* **39**, 29–60.

Wänke, H., Dreibus, G. & Jagoutz, E. (1984). Mantle chemistry and accretion history of the Earth. In: Kröner, A. (ed.) *Archean Geochemistry*. Springer, pp. 1–24.

Watson, E. B. & Harrison, T. M. (2005). Zircon thermometer reveals minimum melting conditions on earliest Earth. *Science* **308**, 841–844.

Wilde, S. A., Valley, J. W., Peck, W. H. & Graham, C. M. (2001). Evidence from detrital zircons for the existence of continental crust and oceans on the Earth 4·4 Gyr ago. *Nature* **409**, 175–178.

Willbold, M., Elliott, T. & Moorbath, S. (2011). The tungsten isotopic composition of Earth's mantle before the terminal bombardment. *Nature* **477**, 195–198.

Willbold, M., Mojzsis, S. J., Chen, H. W. & Elliott, T. (2015). Tungsten isotope composition of the Acasta Gneiss Complex. *Earth and Planetary Science Letters* **419**, 168–177.

Workman, R. K. & Hart, S. R. (2005). Major and trace element composition of the depleted MORB mantle (DMM). *Earth and Planetary Science Letters* **23**, 53–72.

Zahnle, K. J., Claire, M. W. & Catling, D. C. (2006). The loss of mass-independent fractionation of sulfur due to a Paleoproterozoic collapse of atmospheric methane. *Geobiology* **4**, 271–283.

Zahnle, K., Arndt, N., Cockell, C., Halliday, A., Nisbet, E., Selsis, F. & Sleep, N. H. (2007). Emergence of a habitable planet. *Space Science Reviews* **129**, 35–78.